A Successive Flow Direction Enforcing Algorithm for Optimal Operation of Variable-Impedance FACTS Devices

Xinyang Rui[a], Mostafa Sahraei-Ardakani[a]

[a]*Department of Electrical and Computer Engineering, The University of Utah, 50 S. Central Campus Drive, 84112, Salt Lake City, Utah, USA*

Abstract

This paper presents a novel successive flow direction enforcing (SFDE) algorithm for solving power system operation models with flexible AC transmission system (FACTS) devices. The power flow control capabilities of FACTS devices can improve the utilization of the existing transmission network. However, the added computational complexity of modeling FACTS devices in power system operation models is one of the primary challenges for FACTS deployment. A prominent component is the nonlinearity introduced by variable-impedance FACTS devices to the linear DC power flow equations. According to previous studies, such nonlinearity can be tackled by preassigning the power flow directions on lines equipped with FACTS to restore the linearity of DC power flow equations. However, this method has the issue of converging to suboptimal solutions in some cases, due to suboptimal flow direction assignment. The algorithm presented in this paper can address the issue of suboptimality, while still achieving computational efficiency improvements. Power system operation models with FACTS are solved iteratively with flow directions enforced, and the predetermined flow directions are adjusted successively based on the results of the previous iteration. Simulation studies confirm the effectiveness of the method in converging to the globally optimal solution within a few iterations in almost all practical cases.

Keywords: Power flow control, FACTS devices, power system operation, DC power flow.

Nomenclature

Indices

g Index of generators, $g \in G$

k Index of transmission lines, $k \in K$

n Index of buses, $n \in N$

*This document is the results of the research project funded by the National Science Foundation grant number 1756006.

t Index of time periods, $t \in T$

Parameters

b_k Susceptance of line k ($k \notin \mathcal{F}$)

c_g Linear cost of generator g

$d_n(d_{nt})$ Demand at bus n (in time period t)

DT_g Minimum down time of generator g

$f_k^{\max}$ Capacity of line k

FC_{C} Capacitive FACTS capacity

FC_{L} Inductive FACTS capacity

M A very large positive number

N_{F} The number of FACTS devices in the system

NL_g No-load cost of generator g

$p_g^{\max}$ Maximum generator output of generator g

$p_g^{\min}$ Minimum generator output of generator g

RD_g Ramp-down limit of generator g

RU_g Ramp-up limit of generator g

SU_g Start-up cost of generator g

UT_g Minimum up time of generator g

x_k Reactance of line k ($k \notin \mathcal{F}$)

Sets

$\delta^+(n)$ Set of lines that are connected "to" bus n

$\delta^-(n)$ Set of lines that are connected "from" bus n

$\mathcal{F}$ Set of lines equipped with FACTS, $\mathcal{F} \subset K$

$G(n)$ Set of generators connected to bus n

G Set of generators

K Set of transmission lines

N Set of buses

T Set of time periods

Variables

$\theta_{k,\mathrm{fr},t}$ Bus voltage angle at the "from" bus of line k in time period t

$\theta_{k,\mathrm{fr}}$ Bus voltage angle at the "from" bus of line k

$\theta_{k,\mathrm{to},t}$ Bus voltage angle at the "to" bus of line k in time period t

$\theta_{k,\mathrm{to}}$ Bus voltage angle at the "to" bus of line k

b_k Susceptance of line k ($k \in \mathcal{F}$)

$f_k(f_{kt})$ Active power flow on line k (in time period t)

u_{gt} Commitment of generator g in time period t

v_{gt} Start-up of generator g in time period t

x_k Reactance of line k ($k \in \mathcal{F}$)

$z_k(z_{kt})$ Power flow direction on line k (in time period t)

1. Introduction

The annual revenue of the US electric power industry is more than 390 billion dollars [1]. As a result, it is important to improve the efficiency in power system operation. One of the causes of system inefficiency is congestion in transmission systems. Congestion occurs when power transfers reach or exceed the capacity of the existing transmission network [2]. Transmission congestion costs electricity consumers billions of dollars each year across the country [3]. Therefore, it is essential to enhance the transfer capability of transmission systems to address the congestion problem. Sufficient available transfer capability (ATC) should be guaranteed to maintain secure and economical system operation [4]. Besides, insufficient transfer capability is one of the challenges for the integration of higher levels of renewable energy into the power grid [5]. The integration of renewable energy sources (RES) is growing rapidly in the electricity sector and projected to support 36% of power demand worldwide in 2030 [6]. Additionally, the US has an ambitious goal of reaching a carbon-free grid by 2035 [7]. Increased penetration from RES will require further enhancement of transfer capability in the upcoming years.

One obvious approach to enhance transfer capability is upgrading and expanding the transmission system. However, this option is not attractive due to its lengthy process and high level of required investment. Improving utilization of the existing system is a faster and cheaper alternative, even though it cannot completely replace the need for new transmission lines. Regardless, utilization of the existing transmission system to its full capability is always paramount [8]. Utilization improvement can be achieved through the power flow control capabilities provided by the implementation of flexible AC transmission system (FACTS) technologies in the transmission network. It is worth noting that FACTS technology is a non-transmission alternative aligned with FERC order 1000 [9]. With power flow control, power can be rerouted to lines that are not congested to avoid transmission bottlenecks.

FACTS devices are power electronic devices that have the ability to control a variety of system properties, including voltage magnitude, voltage phase angle, shunt susceptance, and impedance of transmission lines [10], thus allowing them to have vital roles

in various domains of power system operation and control [11]. With the fast operation and flexibility, they can be used to dampen low-frequency oscillation and deviations of wind power production [12], [13]. FACTS devices can also help improve reliability and transient stability [14], as well as reduce loop flows in transmission systems [15].

There have already been deployment and planning of FACTS technology in the transmission network in the US and around the world. FACTS technology from Smart Wires Inc., a company that provides modular power flow control solutions, has been deployed in both the Tennessee Valley Authority and Southern Company networks to manage power flow, maintain reliability, and help integrate higher levels of renewable generation [16]. The UPFC Plus devices developed by Siemens can offer power flow capabilities in high-voltage transmission networks with desirable features such as fast response time. General Electric (GE) has deployed series compensation systems in Texas, Vietnam, and the California-Oregon Intertie to help increase transfer capability of existing transmission lines, improve reliability, and, thus, allowing higher level of renewable generation integration [17]. Following a $20 million contract signed in 2018, ABB has planned to install series compensation devices in the vicinity of Brasilia, Brazil to increase transmission capacity while maintaining system stability [18].

This paper focuses on variable-impedance FACTS devices, which has the ability to continuously regulate the reactance of transmission lines, in order to control active power flow [19]. DC power flow is, thus, a good approach for solving the planning and operation problems of variable-impedance FACTS devices. Devices such as the static var compensator (SVC) and the static synchronous compensator (STATCOM) are beyond the scope of this paper as proper modeling of voltage and reactive power is essential for their applications in voltage regulation and reactive power compensation. For the rest of this paper, we use the term "FACTS" to only refer to the types of devices that can provide continuous reactance adjustments with fixed variation limits, such as the thyristor-controlled series compensator (TCSC) and the continuously variable series reactor (CVSR). There are also modular-FACTS (M-FACTS) devices of such type deployed in the power grid, e.g., the PowerLine Guardian device by SmartWires Inc. [20]. Details about FACTS modeling in DC power flow are presented in Section 2.

The ability of FACTS devices to improve transfer capability is well-recognized [21]. However, the utilization of FACTS technology is still limited due to multiple reasons including the legacy operational philosophies that prefer minimal changes to the existing system, cost of devices, and the lack of economic incentives [21], [22]. One main barrier is the computational complexity that FACTS devices introduce to the DC power flow equation. DC-based models are widely used in clearing day-ahead and real-time markets, contingency screening, transmission load relief, transfer capability analysis, and transmission planning [21], [23]. Inclusion of FACTS devices adds nonlinearity to the DC power flow equation, which is linear in its original form. The nonlinearity makes solving power system operation models challenging within the limited time that is available to power system operation software [22].

Previous studies have proposed a mixed-integer reformulation of the DC power flow equation with FACTS included to eliminate the aforementioned nonlinearity [8], [22], [24]. Details of the reformulation is presented in Section 2. In this reformulation, if the flow directions or the signs of bus phase angle differences on transmission lines equipped with FACTS devices are known, the integer variables introduced by the reformulation in power flow equations are eliminated, thus further improving computational efficiency.

Based on such reformulation, a two-stage linear program (LP) method is proposed in [8] to solve DC optimal power flow (DCOPF) with FACTS included, which is an nonlinear program (NLP) originally. In this method, the power flow directions can be obtained by solving a base case DCOPF problem (referred to as OPF_base for simplicity in this paper) that involves no FACTS device. Then, based on a key assumption that FACTS devices are often installed on transmission bottlenecks where the flow direction is unlikely to change [8], the results from OPF_base can be used to predetermine the flow directions, on the lines equipped with FACTS, to construct a second-stage linear program (LP) with FACTS devices included. We refer to this approach as the two-stage method as the two-stage method for the rest of this paper. The two-stage method is also implemented with large-scale systems in [25], where a DCOPF formulation with power transfer distribution factors (PTDF) is proposed, which eliminates the need for calculating bus voltage angles. Although simulation studies reveal impressive improvements in computational efficiency provided by the two-stage method, the issue of suboptimality exists in some cases as the power flow direction results from OPF_base can be suboptimal for formulating the second stage LP with FACTS. Furthermore, the two-stage method has been used in unit commitment (UC) models as well. In [26], the authors applied the two-stage method to solve a stochastic security-constrained unit commitment (SCUC) model, where a base case SCUC is solved for determining the flow directions on lines equipped with FACTS. However, no discussion on the optimality of the solutions and computational efficiency is provided.

Reviewing the two-stage method in the existing literature shows that there is a need for improving the flow direction enforcing approach to address the suboptimality issues, when solving power system operation models with FACTS included, while still providing computational efficiency gains. Additionally, the solution quality when applying the flow direction enforcing approach for UC models needs to be further analyzed. To fill these research gaps, this paper makes the following contributions.

- A novel successive flow direction enforcing (SFDE) algorithm is presented in this paper. The SFDE algorithm addresses the aforementioned suboptimality issue, while still providing computational efficiency improvements over directly solving the power system operation models with FACTS included. The first step of the SFDE algorithm is to initialize the flow directions of transmission lines equipped with FACTS devices. Then, the power system operation models are solved iteratively, with a simple check used to adjusts the enforced line flow directions based on the solution of the previous iteration. Simulation studies with different test systems show that the method converges within a limited number of iterations, and global optimality is achieved in almost all cases.

- The proposed SFDE algorithm is employed to solve more complicated UC model in this paper. Discussion on the solution quality and computational efficiency is presented, thus facilitating expanding the scope of application of the flow direction enforcing approach to UC-based models.

Note that energy and market management system software tools all rely on linear and mixed-integer linear optimization models, using one or another form of DC power flow. Therefore, the SFDE algorithm as a linear method provides compatibility with existing software tools, allowing for straightforward industry adoption.

The rest of this paper is organized as follows. Section 2 presents the methodology. Section 3 includes simulation studies that confirm the effectiveness of the developed method. A discussion on the convergence to optimality is presented in Section 4. Finally, Section 5 concludes this paper.

2. Methodology

The SFDE algorithm is proposed to solve power system operation models with FACTS included. Therefore, FACTS modeling, problem formulations, and the aforementioned mixed-integer reformulation are crucial for presenting the SFDE algorithm, and are, thus, presented first in this section. We then show the idea behind the design of the SFDE algorithm and its detailed steps.

2.1. FACTS modeling

In this paper, the parameter FACTS capacity is used to describe the compensation level of variable-impedance FACTS devices. For any line with FACTS installed, assuming positive line reactance, we have:

$$f_k - b_k(\theta_{k,\text{to}} - \theta_{k,\text{fr}}) = 0, \forall k \in \mathcal{F}; \tag{1}$$

$$b_k^{\min} \leq b_k \leq b_k^{\max}, \forall k \in \mathcal{F}; \tag{2}$$

$$b_k^{\min} = -\frac{1}{(1-FC_{\text{C}})x_k}, \forall k \in \mathcal{F}; \tag{3}$$

$$b_k^{\max} = -\frac{1}{(1+FC_{\text{L}})x_k}, \forall k \in \mathcal{F}. \tag{4}$$

(1) is the DC power flow equation for any transmission line with FACTS. (2) specifies that b_k is a continuous variable with variation limits calculated as in (3) and (4). Devices such as the TCSC and the CVSR provide continuous adjustments of transmission line reactance. The effective susceptance adjustments are within fixed operating ranges. Therefore, (1)–(2) is a proper model for such types of devices. Note that the reactance adjustment levels depend on the actual devices deployed.

2.2. Problem formulations

Due to the bilinear terms $b_k\theta_{k,\text{to}}$ and $b_k\theta_{k,\text{fr}}$, (1) is nonlinear. To address the issue of nonlinearity, (1) and (2) are first reformulated to linear constraints based on the sign of voltage angle differences [22]:

$$\begin{aligned}&\text{if } (\theta_{k,\text{to}} - \theta_{k,\text{fr}}) \geq 0 : \\ &b_k^{\min}(\theta_{k,\text{to}} - \theta_{k,\text{fr}}) \leq f_k \leq b_k^{\max}(\theta_{k,\text{to}} - \theta_{k,\text{fr}}); \end{aligned} \tag{5}$$

$$\begin{aligned}&\text{if } (\theta_{k,\text{to}} - \theta_{k,\text{fr}}) \leq 0 : \\ &b_k^{\max}(\theta_{k,\text{to}} - \theta_{k,\text{fr}}) \leq f_k \leq b_k^{\min}(\theta_{k,\text{to}} - \theta_{k,\text{fr}}). \end{aligned} \tag{6}$$

Binary variables $z_k (z_k \in \{0, 1\})$ are then introduced to model the "if" conditions in (5) and (6) [22]. (1) and (2) can be further reformulated as:

$$b_k^{\min}(\theta_{k,\text{to}} - \theta_{k,\text{fr}}) - (1 - z_k)M \leq f_k, \forall k \in \mathcal{F}; \tag{7}$$

$$b_k^{\max}(\theta_{k,\text{to}} - \theta_{k,\text{fr}}) - z_k M \leq f_k, \forall k \in \mathcal{F}; \tag{8}$$

$$b_k^{\min}(\theta_{k,\text{to}} - \theta_{k,\text{fr}}) + z_k M \geq f_k, \forall k \in \mathcal{F}; \tag{9}$$
$$b_k^{\max}(\theta_{k,\text{to}} - \theta_{k,\text{fr}}) + (1 - z_k)M \geq f_k, \forall k \in \mathcal{F}; \tag{10}$$
$$\theta_{k,\text{to}} - \theta_{k,\text{fr}} \geq (z_k - 1)M, \forall k \in \mathcal{F}; \tag{11}$$
$$\theta_{k,\text{to}} - \theta_{k,\text{fr}} \leq z_k M, \forall k \in \mathcal{F}; \tag{12}$$
$$M > \max_{k \in \mathcal{F}} \{\frac{FC_{\text{C}} + FC_{\text{L}}}{1 - FC_{\text{C}}} f_k^{\max}\}. \tag{13}$$

Note that (13) specifies how the value of M should be set and is not a constraint as M is a parameter. In (7)-(12), z_k represents the flow direction on transmission line $k(k \in \mathcal{F})$ in the following manner:

$$z_k = 0 \iff f_k \geq 0, \tag{14}$$
$$z_k = 1 \iff f_k < 0. \tag{15}$$

The reformulation of (1)–(2) to (7)-(12) is the previously discussed mixed-integer reformulation of DC power flow equation for lines with FACTS installed using the big-M method [8, 22, 24]. The full formulation of DCOPF with FACTS (OPF_FACTS) after applying this reformulation is presented as follows:

OPF_FACTS :

$$\min \sum_{g \in G} c_g p_g \tag{16}$$

s.t.

$(7) - (13)$;

$$p_g^{\min} \leq p_g \leq p_g^{\max}, g \in G; \tag{17}$$
$$-f_k^{\max} \leq f_k \leq f_k^{\max}, k \in K; \tag{18}$$
$$f_k = b_k(\theta_{k,\text{to}} - \theta_{k,\text{fr}}), k \notin \mathcal{F}, k \in K; \tag{19}$$
$$\theta_1 = 0; \tag{20}$$
$$\sum_{k \in \delta^+(n)} f_k - \sum_{k \in \delta^-(n)} f_k + \sum_{g \in G(n)} p_g = d_n, n \in N. \tag{21}$$

The objective is to minimize the total fuel cost of generators and is calculated using the linear function shown in (16). The generator operating capacities are specified in (17). (18) imposes thermal capacity limits on transmission lines. (19) is the DC power flow equation for lines without FACTS. (20) specifies that the voltage angle of the reference bus equals to zero. (21) represents the nodal power balance constraint at all the buses of the network.

Similarly, we can formulate the more complicated UC model with FACTS included (UC_FACTS). The formulation is presented as follows:

UC_FACTS :

$$\min \sum_{g \in G} \sum_{t \in T} (NL_g u_{gt} + c_g p_{gt} + SU_g v_{gt}) \tag{22}$$

s.t.

$$u_{gt}p_g^{\min} \le p_{gt} \le u_{gt}p_g^{\max}, g \in G, t \in T; \tag{23}$$

$$-f_k^{\max} \le f_{kt} \le f_k^{\max}, k \in K, t \in T; \tag{24}$$

$$f_k = b_k(\theta_{k,\mathrm{to},t} - \theta_{k,\mathrm{fr},t}), k \notin \mathcal{F}, k \in K, t \in T; \tag{25}$$

$$\frac{\theta_{k,\mathrm{fr},t} - \theta_{k,\mathrm{to},t}}{(1+FC_{\mathrm{L}})x_k} - z_{kt}M \le f_{kt}, k \in \mathcal{F}, t \in T; \tag{26}$$

$$\frac{\theta_{k,\mathrm{fr},t} - \theta_{k,\mathrm{to},t}}{(1-FC_{\mathrm{C}})x_k} - (1-z_{kt})M \le f_{kt}, k \in \mathcal{F}, t \in T; \tag{27}$$

$$\frac{\theta_{k,\mathrm{fr},t} - \theta_{k,\mathrm{to},t}}{(1+FC_{\mathrm{L}})x_k} + (1-z_{kt})M \ge f_{kt}, k \in \mathcal{F}, t \in T; \tag{28}$$

$$\frac{\theta_{k,\mathrm{fr},t} - \theta_{k,\mathrm{to},t}}{(1-FC_{\mathrm{C}})x_k} + z_{kt}M \ge f_{kt}, k \in \mathcal{F}, t \in T; \tag{29}$$

$$\theta_{k,\mathrm{to},t} - \theta_{k,\mathrm{fr},t} \le z_{kt}M, k \in \mathcal{F}, t \in T; \tag{30}$$

$$\theta_{k,\mathrm{to},t} - \theta_{k,\mathrm{fr},t} \ge (z_{kt}-1)M, k \in \mathcal{F}, t \in T; \tag{31}$$

$$z_{kt} \in \{0,1\}, k \in \mathcal{F}, t \in T; \tag{32}$$

$$M > \max_{k \in \mathcal{F}}\{\frac{FC_{\mathrm{C}} + FC_{\mathrm{L}}}{1-FC_{\mathrm{C}}} f_k^{\max}\}; \tag{33}$$

$$\theta_{1t} = 0, t \in T; \tag{34}$$

$$\sum_{k \in \delta^+(n)} f_{kt} - \sum_{k \in \delta^-(n)} f_{kt} + \sum_{g \in G(n)} p_{gt} = d_{nt}, n \in N, t \in T; \tag{35}$$

$$-RD_g \le p_{g,t+1} - p_{gt} \le RU_g, g \in G, t \in T; \tag{36}$$

$$\sum_{r=t-UT_g+1}^{t} v_{gr} \le u_{gt}, g \in G, t \ge UT_g; \tag{37}$$

$$\sum_{r=t+1}^{t+DT_g} v_{gr} \le 1 - u_{gt}, g \in G, t \le |T| - DT_g; \tag{38}$$

$$0 \le v_{gt} \le 1, g \in G, t \in T; \tag{39}$$

$$u_{gt} - u_{g,t-1} \le v_{gt}, g \in G, t \in T; \tag{40}$$

$$u_{gt} \in \{0,1\}, g \in G, t \in T;. \tag{41}$$

(22) is the objective function of the UC problem, which minimizes the summation of fuel cost, start-up cost, and no-load cost of the generators. The constraints (23)–(34) are similar to (17)–(20) and (7)–(13), with differences being the commitment variables in (23) and the time indices. (35) represents the nodal power balance constraints. The ramping constraints of generators are specified in (36). (37)–(38) represent the minimum up and down time constraints. (39) defines the upper and lower bounds of start-up variables. (40) represents the relationship between commitment variables and start-up variables. (41) specifies that commitment variables are binary. Note that start-up variables are continuous in this formulation, as they will converge to the bounds shown in (39) in the final solutions.

The power flow directions on lines equipped with FACTS can be assigned by determining the values of z_k in (7)–(12) and z_{kt} in (26)–(31), thus eliminating these binary

variables and consequently improving computational efficiency. The results of a base case, which is a DCOPF or UC model without any FACTS device, can be used to predetermine the flow directions. The full formulations of the base cases (OPF_base and UC_base) are presented as follows:

OPF_base :

$$\min \sum_{g \in G} c_g p_g \tag{42}$$

s.t.

$$(17) - (18), (20) - (21);$$

$$f_k = b_k(\theta_{k,\text{to}} - \theta_{k,\text{fr}}), k \in K, \tag{43}$$

UC_base :

$$\min \sum_{g \in G} \sum_{t \in T} (NL_g u_{gt} + c_g p_{gt} + SU_g v_{gt}) \tag{44}$$

s.t.

$$(23) - (24), (34) - (41);$$

$$f_{kt} = b_k(\theta_{k,\text{to},t} - \theta_{k,\text{fr},t}), k \in K, t \in T. \tag{45}$$

2.3. SFDE algorithm design

As mentioned previously, the base case solutions can provide suboptimal flow directions for solving the power system operation model with FACTS included. Therefore, the two-stage method presented in [8] may suffer from suboptimaility in the final solution. The SFDE algorithm addresses the suboptimality issue by adjusting the enforced flow directions. The idea behind the design of the SFDE algorithm is first discussed in this subsection. Two versions of the SFDE algorithm that serve different purposes in the simulation studies are then presented.

The idea behind the SFDE algorithm is based on analyzing the feasible set identified from constraints (1) and (2) regarding f_k and $\Delta\theta_k = \theta_{k,\text{to}} - \theta_{k,\text{fr}}$, as shown in Fig. 1 [27].

The feasible set can be divided into two halves that are symmetric around the origin. Note that the sign of voltage angle difference determines the direction of power flow. By initializing the power flow direction, we are limiting the feasible set to only one of the halves. If the predetermined flow direction limits the feasible set to the suboptimal segment, the solution is expected to converge to the origin in Fig. 1, which is the point that connects the two halves of the feasible set and leads to the power flow being zero on the corresponding line. Based on this reasoning, once such a result is identified in the initial solution, or any iteration thereafter, we can change the direction of the power flow to the opposite of the previous iteration and proceed to a new iteration. Simulation results show that within just a few iterations of adjusting the enforced power flow directions and solving the power system operation problems, the SFDE algorithm converges to the globally optimal solution in almost all practical cases.

The two important aspects regarding the performance of the SFDE algorithm are (i) convergence to global optimality and (ii) computational efficiency. We first traverse all

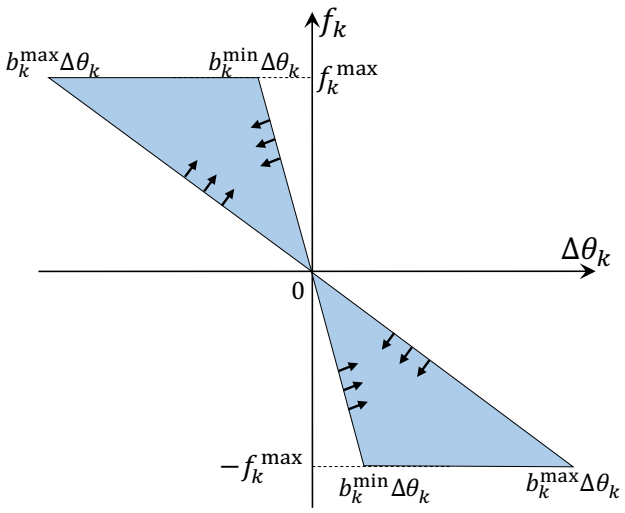

Figure 1: The feasible set of power flow on transmission line k ($k \in \mathcal{F}$) [27]

possible initializations of power flow directions. Doing so allows us to create a variety of cases to demonstrate the effectiveness of SFDE in converging to global optimality. The SFDE algorithm with random initialization of flow directions is presented as follows:

Algorithm 1 The SFDE algorithm with random initialization of flow directions

1: *Initialization*–Randomly initialize power flow directions on lines with FACTS. Create $\Omega = \emptyset$;
2: *Parallel lines flow direction check*–If opposite directions are initialized on parallel lines, go back to step 1. If not, continue;
3: *Solve*–Solve the operation model with enforced flow directions;
4: *Feasibility check*–If this initialization of power flow directions causes infeasibility, go back to step 1. If not, record the result β and continue;
5: *Zero flow value check*–If active power flow results on lines with FACTS installed do not contain zero, go to step 8;
6: *Same results check*–IF $\beta \in \Omega$, go to step 8. If not, $\Omega = \{\beta\} \cup \Omega$;
7: *Enforced flow direction adjustment*–If a line with FACTS installed has a power flow with value of zero, flip the enforced direction. Go back to step 3;
8: *Report and end*–Report the final results and end the algorithm.

It is worth noting that while traversing all possible power flow direction initializations, the results reveal that an arbitrary initialization of power flow directions does not guarantee feasibility. In fact, the majority of the initializations lead to infeasibility. The explanation is that based on the locations of the generating units and load in the system, forcing the flow directions on some transmission lines to be fixed may result in constraints that cannot be satisfied. In other words, changing the dispatch may not be able to change the flow direction on certain transmission lines.

In addition, there are multiple pairs of parallel lines connecting the same pair of buses

in the test systems we use. Flow directions on parallel lines should not be initialized as opposite. Even though some of the cases where the flow directions on parallel lines are initialized as different are still feasible, the solutions are not optimal, and thus not useful. Feasibility in those cases are achieved only if the flow on the parallel lines, forced to have opposite flow directions, is zero. Such cases are eliminated when identified after initialization in our simulations.

In the actual implementation of SFDE, results of the base case, or state estimation, can be used for flow direction initialization to guarantee feasibility and improve computational performance. The SFDE algorithm with warm-start (Algorithm 2) is presented as follows:

Algorithm 2 The SFDE algorithm with warm-start

1: *Warm-start*–Solve a base case and enforce power flow directions on lines with FACTS installed based on the results and create $\Omega = \emptyset$;
2: *Solve*–Solve the operation model with enforced flow directions and record the result β;
3: *Zero flow value check*–If active power flow results on lines with FACTS installed do not contain zero, go to step 6;
4: *Same results check*–If $\beta \in \Omega$, go to step 8. If not, $\Omega = \{\beta\} \cup \Omega$;
5: *Enforced flow direction adjustment*–If a line with FACTS installed has a power flow with value of zero, flip the enforced direction. Go back to step 2;
6: *Report and end*–Report the final results and end the algorithm.

Compared to Algorithm 1, the step of parallel line flow direction checking is spared in Algroithm 2 as the base case solution will not have opposite flow directions on parallel lines. Both Algorithm 1 and Algorithm 2 stops when no power flow result is zero and no further adjustments of flow directions can be made. In addition, the design of both algorithms involve creating the set of Ω to record the result of each iteration. Then, in the later step of same results checking, exit the algorithm if the same result reappears. This design is to ensure an exit condition when the optimal solution involves zero power flows on lines equipped with FACTS. Due to the MIPgap in UC problems the results in the heuristic will show a cycling behavior. Therefore, it is necessary to record the results of each iteration.

In the simulation studies presented in Section 3, the SFDE algorithm is applied to solve OPF_FACTS and UC_FACTS. The total cost result will be compared to that of directly solving OPF_FACTS and UC_FACTS to show that the SFDE algorithm's convergence to global optimality. A comparison is also drawn between the solution time results to show that the SFDE algorithm provides computational efficiency improvements over directly solving OPF_FACTS and UC_FACTS.

3. Simulation Studies

In this section, the method proposed in Section 2 is employed to solve power system operation models OPF_FACTS and UC_FACTS. The test system used are the modified IEEE 118-bus system and the Texas 2000-bus system. Simulation results are presented to

show the effectiveness of our algorithm. The effectiveness is evaluated through comparison with results of directly solving OPF_FACTS and UC_FACTS to see if the proposed method (i) has achieved optimality and (ii) can provide computational efficiency gains. Problems are solved using CPLEX 12.10 on an Intel Xeon Gold 6136 CPU with 128 GB RAM.

3.1. Implementation of SFDE for solving OPF_FACTS

We first implement the SFDE algorithm to solve OPF_FACTS. OPF_FACTS being a single-hour operation model allows us to implement Algorithm 1 when N_{F} is relatively small, thus, as mentioned previously, creating a variety of flow direction initializations to demonstrate the effectiveness of the SFDE algorithm in converging to optimality. Because of the presence of binary variables, OPF_FACTS is a mixed-integer linear program (MILP). In each iteration of the SFDE algorithm, the binary variables are effectively eliminated, thus LPs are being solved successively.

To demonstrate the robustness and effectiveness of the proposed algorithm under different FACTS device allocation schemes, we use two allocation policies (AP) which are presented as follows:

- AP1: FACTS devices are located on each of lines that are utilized the most;
- AP2: FACTS devices are located on each of the lines with larger reactance.

Note that optimal allocation of FACTS devices is beyond the scope of this paper. We apply the two aforementioned simple, straightforward APs for the following reasons:

1. The most utilized lines in the system are very likely transmission bottlenecks. Therefore, FACTS devices deployed on these lines can "push power flow away" by increasing the line reactance, thus alleviate congestion;
2. FACTS devices deployed on the lines with higher reactance can reduce the reactance of these lines, thus "pull power flow in" to reduce congestion.

For FACTS capacity, the following settings are employed in simulation studies:

- Setting 1: $FC_{\mathrm{C}} = FC_{\mathrm{L}} = 0.5$;
- Setting 2: $FC_{\mathrm{C}} = 0.8, FC_{\mathrm{L}} = 0.2$;

Each of these settings are typical operating ranges of the widely used TCSC devices [28].

3.1.1. Modified IEEE 118-bus system

Algorithm 1 is first employed to solve OPF_FACTS for the modified IEEE 118-bus test system. The data is obtained from [29]. Because of the low congestion level in the original test system, modifications are made to thermal capacities of the most utilized lines to increase congestion, making the system more suitable for studying the impact of FACTS deployment. Details of the modifications are presented in the Appendix.

Note that for each line k equipped with FACTS there are two initializations for power flow direction, corresponding to z_k in (7)-(12) taking the value of 1 or 0. As a result, there are $2^{N_{\mathrm{F}}}$ possible initializations of power flow directions on lines equipped with FACTS, which are traversed in the simulations. The number of feasible cases and

average iterations in SFDE for each FACTS capacity setting is presented in the results. The average number of iterations presents the average number of LPs solved including solving the case with the flow direction initialization. Each "case" refers to a way that the power flow directions are initialized in Algorithm 1. The simulation results when 5 FACTS are installed in the system are presented in Table 1–2.

Table 1: Simulation results of Algorithm 1 with 5 FACTS devices under AP1 in the 118-bus system

FACTS Setting	**# Feasible Cases**	**Average # Iterations**	**Cost ($/h)**	**OPF_FACTS Cost ($/h)**
1	10	1.9	60548.3	60548.3
2	8	1.86	60749.6	60749.6

Table 2: Simulation results of Algorithm 1 with 5 FACTS devices under AP2 in the 118-bus system

FACTS Setting	**# Feasible Cases**	**Average # Iterations**	**Cost ($/h)**	**OPF_FACTS Cost ($/h)**
1	14	2.71	60745.7	60745.7
2	14	2.71	60588.7	60588.7

The simulation results when 10 FACTS are installed in the 118-bus system are presented in Table 3 and 4. More savings can be achieved with a larger number of FACTS devices installed.

Table 3: Simulation results of Algorithm 1 with 10 FACTS devices under AP1 in the 118-bus system

FACTS Setting	**# Feasible Cases**	**Average # Iterations**	**Cost ($/h)**	**OPF_FACTS Cost ($/h)**
1	40	1.97	60393.8	60393.8
2	36	1.98	60557.7	60557.7

Table 4: Simulation results of Algorithm 1 with 10 FACTS devices under AP2 in the 118-bus system

FACTS Setting	**# Feasible Cases**	**Average # Iterations**	**Cost ($/h)**	**OPF_FACTS Cost ($/h)**
1	136	2.4	60698.9/60699.2	60698.9
2	136	3.4	60532.9	60532.9

We implement Algorithm 2 instead of Algorithm 1 when N_F is increased to 15 as it is impractical to traverse 2^{15} initializations. The results are presented in Tables 5–6.

We first discuss the effectiveness of the SFDE algorithm in converging to the same result as that of directly solving OPF_FACTS. Tables 1–6 include 389 feasible cases in total, out of which, 309 (79.4%) have succefully converged to the same result compared to that of OPF_FACTS. The exceptions occur with 10 FACTS devices of setting 1 deployed in the system under AP2 and results can be seen from Table 4. In these specific cases, 80 out of 136 feasible cases resulted in suboptimal results. However, we can see that the

Table 5: Simulation results of Algorithm 2 with 15 FACTS devices under AP1 in the 118-bus system

FACTS Setting	# Iterations	Cost ($/h)	OPF_FACTS Cost ($/h)
1	1	60378.2	60378.2
2	1	60550.5	60550.5

Table 6: Simulation results of Algorithm 2 with 15 FACTS devices under AP2 in the 118-bus system

FACTS Setting	# Iterations	Cost ($/h)	OPF_FACTS Cost ($/h)
1	1	60688.9	60688.9
2	2	60517.1	60517.1

suboptimality is \$0.3 (0.0005%) which is very minimal. The suboptimality occurs due to the nonconvexity of the feasible region shown in Fig. 1. A more detailed discussion of the limitation of the proposed algorithm is presented in Section 4. Overall, the results with the 118-bus system demonstrated the effectiveness of the SFDE algorithm in converging to global optimality in most of the practical cases even with random flow direction initialization in a limited number of iterations.

We then present the comparison of the average solution time results between applying the SFDE algorithm and directly solving OPF_FACTS. The results are presented in Fig. 2.

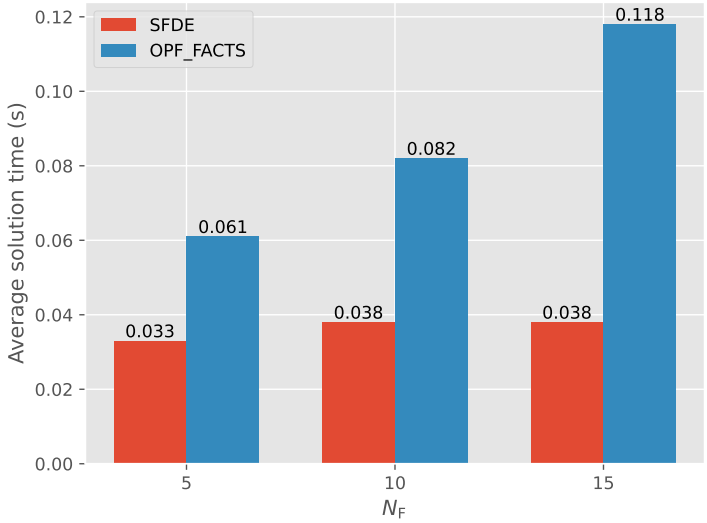

Figure 2: Solution time of the SFDE algorithm and directly solving OPF_FACTS with the 118-bus system

Table 7 shows the computational efficiency superiority of the SFDE algorithm over directly solving OPF_FACTS.

Table 7: Computational efficiency superiority of the SFDE algorithm over directly solving OPF_FACTS for the 118-bus system

N_F	Computatonal efficiency improvement
5	84.1%
10	115.8%
15	210.5%

We can see that employing the SFDE algorithm is significantly more efficient than directly solving OPF_FACTS. The two factors contributing to such computational efficiency gain are (i) the LP in each iteration is much less computationally demanding than the MILP and (ii) the SFDE algorithm is capable of converging within a few iterations. Furthermore, higher computational efficiency gain is shown with more FACTS devices deployed in the system.

Note that the computational efficiency improvement results are based on the total solution time reported by the solver. The solvers require a certain amount of time to construct the construct the optimization models. The model construction time is reported in this section as they are much smaller than the solution time, especially for complicated models. Additionally, the model construction time varies when using different programming languages.

3.1.2. Texas 2000-bus system

The Texas 2000-bus test system is first introduced in [30], and the data is available from [31]. Similar to the 118-bus system, modifications are made to the 2000-bus system to increase congestion so that it is more suitable for studying the influence of FACTS devices. Details of the modifications of the system are shown in the Appendix.

The 2000-bus system has 3206 transmission lines, which is significantly more than the 186 lines in the 118-bus system. Therefore, if we keep the number of FACTS devices the same in the 2000-bus system, the number of binary variables is scaling significantly less than the LP in each SFDE iteration. To better demonstrate the effectiveness of the proposed algorithm, we increased N_F to 45, 60, and 75 for the 2000-bus system. Note that such deployment can be carried out cost-efficiently and conveniently through distributed or modular FACTS (D-FACTS or M-FACTS), which is a light-weight version of FACTS devices [32] that offers better cost-effectiveness and re-allocation flexibility compared to conventional FACTS technologies [33].

As N_F is large for the 2000-bus system, Algorithm 2 is applied in this part of the simulation studies. Results of a total of 12 cases are included in Tables 8–13.

Table 8: Simulation results of Algorithm 2 with 45 FACTS devices under AP1 in the 2000-bus system

FACTS Setting	# Iterations	Cost ($/h)	OPF_FACTS Cost ($/h)
1	1	889613.4	889613.4
2	1	891347.4	891347.4

Table 9: Simulation results of Algorithm 2 with 45 FACTS devices under AP2 in the 2000-bus system

FACTS Setting	# Iterations	Cost ($/h)	OPF_FACTS Cost ($/h)
1	3	908929.7	908929.7
2	4	908563.5	908563.5

Table 10: Simulation results of Algorithm 2 with 60 FACTS devices under AP1 in the 2000-bus system

FACTS Setting	# Iterations	Cost ($/h)	OPF_FACTS Cost ($/h)
1	2	884754.2	884754.2
2	2	887654.5	887654.5

Table 11: Simulation results of Algorithm 2 with 60 FACTS devices under AP2 in the 2000-bus system

FACTS Setting	# Iterations	Cost ($/h)	OPF_FACTS Cost ($/h)
1	3	908866.2	908866.2
2	3	908522.9	908532.6

Table 12: Simulation results of Algorithm 2 with 75 FACTS devices under AP1 in the 2000-bus system

FACTS Setting	# Iterations	Cost ($/h)	OPF_FACTS Cost ($/h)
1	2	884752.2	884752.2
2	2	887652.2	887652.2

Table 13: Simulation results of Algorithm 2 with 75 FACTS devices under AP2 in the 2000-bus system

FACTS Setting	# Iterations	Cost ($/h)	OPF_FACTS Cost ($/h)
1	3	908810.9	908810.9
2	3	908429.7	908532.6

The results reveal the effectiveness of the SFDE algorithm to converge to global optimality after very few iterations of solving successive LPs in a large system with a

significantly larger N_{F}. Note that the number of iterations shown in Tables 8–13 does not include solving the base case. The results also show consistency with the simulation results in Section 3.1.1: a larger N_{F} or greater FACTS capacity can lead to higher savings.

The solution time comparison between the SFDE algorithm and directly solving OPF_FACTS is presented in Fig. 3, and Table 14 shows the computational efficiency superiority of the SFDE algorithm over solving OPF_FACTS for the 2000-bus system.

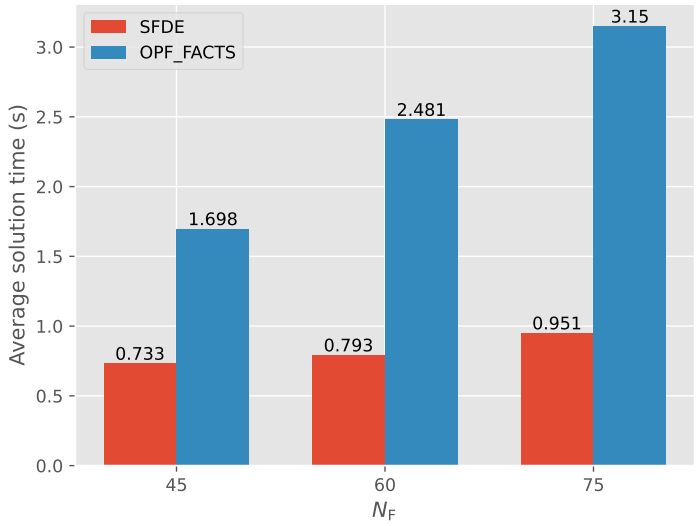

Figure 3: Solution time of the SFDE algorithm and directly solving OPF_FACTS with the 2000-bus system

Table 14: Computational efficiency superiority of the SFDE algorithm over directly solving OPF_FACTS with the 2000-bus system

$\boldsymbol{N_{\mathrm{F}}}$	**Computational efficiency improvement**
45	131.7%
60	212.9%
75	231.2%

The results again shows the significant computational efficiency improvement when the SFDE algorithm is applied, which is consistent with the results obtained using the 118-bus system. It is worth noting that even though the number of FACTS deployment is increased in the 2000-bus system, the lines equipped with FACTS devices is still a very small portion of the lines in the system. With the development of M-FACTS technology, a greater number of FACTS devices deployed in the system can be expected. The computational efficiency of the SFDE algorithm can be expected to be even more

valuable under these circumstances.

3.2. Implementation of SFDE for solving UC_FACTS

In this subsection, we conduct simulation studies to demonstrate the computational efficiency gains provided by the SFDE algorithm, while still converging to global optimality with the UC model. We consider a typical day-ahead UC model with $|T| = 24$. Hourly load data for a winter weekday is obtained from [34]. For the day-ahead UC there are $2^{|T|N_{\mathrm{F}}}$ possible initializations of power flow directsions, and traversing all of them is certainly impractical. Therefore, Algorithm 2 is applied for the UC problems. UC_base is solved and the solutions are used to determine the values of z_{kt}. Because of the significant computational complexity of UC models, the 118-bus system is used in this part of the simulation studies. For brevity, only AP1 and setting 1 are used for UC simulations, and setting 1 is used as it has been shown to be more cost-efficient under this allocation policy by the results in the previous subsection. Simulation results with 5, 10, and 15 devices in the system are presented in Tables 15–17.

Table 15: UC Simulation results of Algorithm 2 with 5 FACTS devices in the 118-bus system

Iteration	**SFDE Cost ($)**	**UC_FACTS Cost ($)**
First	1127676.3	1127177.5
Final (3)	1127331.0	

Table 16: UC Simulation results of Algorithm 2 with 10 FACTS devices in the 118-bus system

Iteration	**SFDE Cost ($)**	**UC_FACTS Cost ($)**
First	1125514.7	1123710.7
Final (4)	1123862.7	

Table 17: UC Simulation results of Algorithm 2 with 15 FACTS devices in the 118-bus system

Iteration	**SFDE Cost ($)**	**UC_FACTS Cost ($)**
First	1125224.1	1123265.3
Final (11)	1123583.0	

In Tables 15–17, the results of both the first iteration and the final iteration of the SFDE algorithm are presented. The cost of the first SFDE iteration is equivalent to the result that would be achieved if the two-stage method proposed in [8] and [26] is employed. The objective function values of the final iterations are the eventual results reported by the SFDE algorithm. We compare both sets of results to the costs achieved by directly solving UC_FACTS, and the differences are shown in Table 18.

Table 18: Comparing the results of the two-stage method and the SFDE algorithm to the result of UC_FACTS

N_F \ Method	Two-stage	SFDE
5	0.044%	0.014%
10	0.161%	0.014%
15	0.174%	0.046%

Note that the MIPgap used for UC problems is 0.1%. Therefore, the results in the "SFDE" column in Table 18 shows the convergence of the SFDE algorithm to optimality, as the difference is smaller than the defined MIPgap. The results of the two-stage method, however, suffer from significant suboptimlity that is equivalent to 161% and 174% of the MIPgap with 10 or 15 FACTS devices deployed in the system. The results in Table 18 reveal the superiority of the SFDE algorithm over the two-stage method in the quality of final solutions.

We then compare the solution time of the SFDE algorithm to that of directly solving UC_FACTS to demonstrate the computational efficiency improvement. The results are presented in Fig. 4 and the computational efficiency gains of the SFDE algorithm are shown in Table 19.

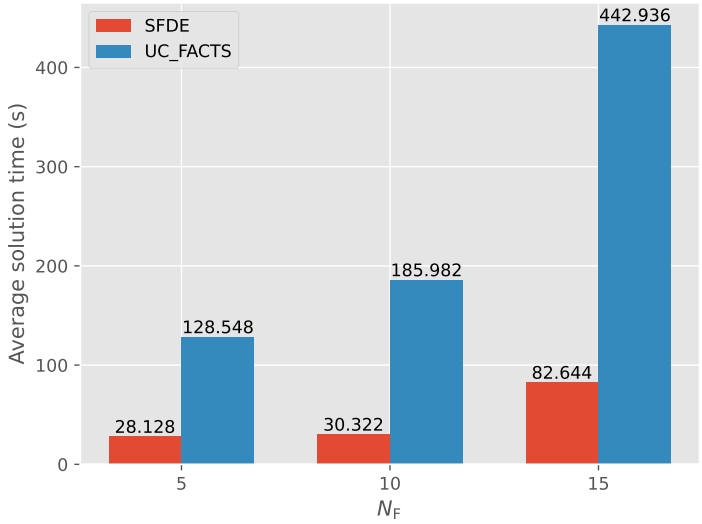

Figure 4: Solution time of the SFDE algorithm and directly solving UC_FACTS

It can be seen that the SFDE algorithm is significantly more efficient than directly solving UC_FACTS. Similar to the results in Section 3.1, the SFDE algorithm shows more computational efficiency superiority with a larger N_F. Note that for $N_F = 15$,

Table 19: Computational efficiency superiority of the SFDE algorithm over directly solving UC_FACTS with the 118-bus system

N_F	Computational efficiency improvement
5	357.0%
10	513.4%
15	536.0%

the SFDE algorithm converges after 11 iterations and still provides huge computational efficiency gain, which shows the significant impact of FACTS operation on computaional complexity, as well as the benefit of alleviating it through flow direction enforcing.

4. Discussion on Convergence

It should be noted that even though simulation studies show the practical effectiveness of the SFDE algorithm, it still does not theoretically guarantee global optimality due to the non-convexity of the problem. Here we present an example in a simple 3-bus system, shown in Fig. 5, to demonstrate the limitation of the algorithm. Variables and parameters are labelled in the figure. For the sake of simplicity, we consider a linear cost function in this example as well.

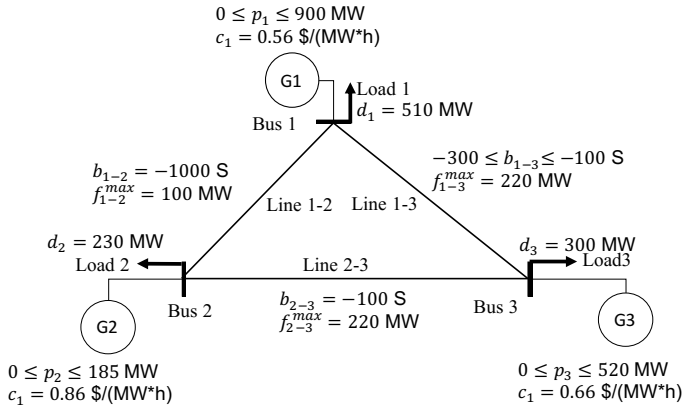

Figure 5: Example in a 3-bus system to demonstrate the mathematical limitation of the SFDE algorithm

Line 3-1 is the only transmission line equipped with FACTS in the above system, which results in two possible ways of initializing of power flow direction on this line when using the algorithm introduced in this paper. The generation dispatch and power flow results in both cases are presented in Table 20.

We can see that if the flow direction on line 3-1 is initialized as from bus 1 to bus 3 in the system, the subsequent LP converges to a suboptimal cost with a non-zero power flow on line 3-1. In this case, the SFDE method will stop and report the solution. This example shows that the method cannot theoretically guarantee global optimality.

Table 20: Results of the counterexample case

Init. / Results	Flow direction on Line 3-1 from 1 to 3	Flow direction on Line 3-1 from 3 to 1
f_{1-2} (MW)	100	100
f_{2-3} (MW)	50	-105
f_{3-1} (MW)	-180	95
p_1 (MW)	780	505
p_2 (MW)	200	45
p_3 (MW)	70	500
Cost ($/h)	642.9	638.9

However, multiple conditions need to be satisfied simultaneously to allow such an example to occur. First, the flow on line 3-1 in this case is very sensitive to changes in dispatch that would keep the total cost constant (i.e., increase of p_3 and decrease of p_1 and p_2, by 2/3 and 1/3 of the increase in p_3). Therefore, two very similar solutions in terms of total cost, can lead to drastically different flows on line 3-1. This is not very likely in real world systems. Moreover, in this example the FACTS device is not placed on line 1-2, which is a better location as it is the most utilized and constrained line in the system. Therefore, we believe it will be rare for the method to converge to a suboptimal solution in a realistically large system with FACTS devices that are properly allocated.

A previous study [35] states that if only one transmission line is equipped with FACTS, the two-stage method in [8] will converge to the globally optimal solution. The example above clearly counters this theorem.

5. Conclusion

FACTS devices can effectively enhance the transfer capability over the existing transmission networks. Unfortunately, however, it has been shown that the inclusion of FACTS devices increases the computational burden of power system operation models. This paper presents a successive flow direction enforcing (SFDE) algorithm to solve power system operation models and optimize FACTS operation. Recent studies have proposed a mixed-integer reformulation of the DC power flow equation with FACTS, which is nonlinear. Based on this reformulation, power flow directions on lines equipped with FACTS can be preassigned to achieve computational efficiency improvements. The SFDE algorithm iteratively adjusts the preassigned flow directions to practically guarantee optimality, thus addressing the suboptimality issue of methods in the existing literature, while providing computational efficiency gains compared to directly solving operation models with FACTS included. Simulation results on different test systems confirm that the proposed SFDE algorithm converges to the globally optimal solution for almost all practical cases within a few iterations. Simulation studies also show that, compared to directly solving power system operation models with FACTS included, implementing the SFDE algorithm can achieve up to 231.2% and 536.0% computational efficiency improvement in for OPF and UC problems respectively.

Due to its linear nature, the algorithm developed in this paper can be integrated within the existing energy and market management systems, without substantially adding to the computational demands of the existing software tools. Even though global optimality is not guaranteed theoretically, the effectiveness of this method is expected to be satisfactory from a practical standpoint.Future work will include employing the proposed algorithm in more complex power system operation and planning models, such as security-constrained optimal power flow (SCOPF) and stochastic unit commitment (SUC).

References

[1] Electric Power Annual 2020, accessed: 2021-12-20 (2021).
URL https://www.eia.gov/electricity/annual/pdf/epa.pdf

[2] M. EL-Azab, W. Omran, S. Mekhamer, H. Talaat, Congestion management of power systems by optimizing grid topology and using dynamic thermal rating, Electric Power Systems Research 199 (2021) 107433.

[3] Y. Sang, M. Sahraei-Ardakani, The link between power flow control technologies: Topology control and FACTS, in: 2017 North American Power Symposium (NAPS), IEEE, 2017, pp. 1–6.

[4] Y. Xiao, Y. Song, C.-C. Liu, Y. Sun, Available transfer capability enhancement using FACTS devices, IEEE transactions on power systems 18 (1) (2003) 305–312.

[5] X. Zhang, D. Shi, Z. Wang, B. Zeng, X. Wang, K. Tomsovic, Y. Jin, Optimal allocation of series FACTS devices under high penetration of wind power within a market environment, IEEE Transactions on power systems 33 (6) (2018) 6206–6217.

[6] M. S. Alam, F. S. Al-Ismail, A. Salem, M. A. Abido, High-level penetration of renewable energy sources into grid utility: Challenges and solutions, IEEE Access 8 (2020) 190277–190299.

[7] White House, FACT SHEET: President Biden sets 2030 greenhouse gas pollution reduction target aimed at creating good-paying union jobs and securing u.s. leadership on clean energy technologies, accessed: 2021-12-20 (April 2021).
URL https://www.whitehouse.gov/briefing-room/statements-releases/2021/04/22/fact-sheet-president-biden-sets-2030-greenhouse-gas-pollution-reduction-target-aimed-at-creating-good-paying-union-jobs-and-securing-u-s-leadership-on-clean-energy-technologies/

[8] M. Sahraei-Ardakani, K. W. Hedman, A fast LP approach for enhanced utilization of variable impedance based FACTS devices, IEEE Transactions on Power Systems 31 (3) (2015) 2204–2213.

[9] Federal Energy Regulatory Commission, Order no. 1000 - transmission planning and cost allocation, accessed: 2018-12-01 (2011).
URL https://www.ferc.gov/electric-transmission/order-no-1000-transmission-planning-and-cost-allocation

[10] Y. Sang, M. Sahraei-Ardakani, The interdependence between transmission switching and variable-impedance series FACTS devices, IEEE Transactions on Power Systems 33 (3) (2017) 2792–2803.

[11] P. Singh, N. Senroy, Steady-state models of statcom and upfc using flexible holomorphic embedding, Electric Power Systems Research 199 (2021) 107390.

[12] W. Yao, L. Jiang, J. Wen, Q. Wu, S. Cheng, Wide-area damping controller of FACTS devices for inter-area oscillations considering communication time delays, IEEE Transactions on Power Systems 29 (1) (2013) 318–329.

[13] A. Nasri, A. J. Conejo, S. J. Kazempour, M. Ghandhari, Minimizing wind power spillage using an OPF with FACTS devices, IEEE Transactions on Power Systems 29 (5) (2014) 2150–2159.

[14] M. M. Eladany, A. A. Eldesouky, A. A. Sallam, Power system transient stability: An algorithm for assessment and enhancement based on catastrophe theory and facts devices, IEEE Access 6 (2018) 26424–26437.

[15] K. Habur, D. O'Leary, FACTS-flexible alternating current transmission systems: for cost effective and reliable transmission of electrical energy, Siemens-World Bank document–Final Draft Report, Erlangen 46 (2004).

[16] Order no. 1000 - transmission planning and cost allocation (2011).
URL https://www.ferc.gov/electric-transmission/order-no-1000-transmission-planning-and-cost-allocation

[17] GE Grid Solutions, Series Compensation Systems, accessed: 2019-09-20 (2015).
URL https://www.gegridsolutions.com/products/brochures/powerd_vtf/seriescompensation_gea12785c_lr.pdf
[18] ABB, ABB to improve power supply and reliability in brazil, accessed: 2019-09-20 (November 2018).
URL https://new.abb.com/news/detail/10072/abb-to-improve-power-supply-and-reliability-in-brazil
[19] S. Gerbex, R. Cherkaoui, A. J. Germond, Optimal location of multi-type FACTS devices in a power system by means of genetic algorithms, IEEE transactions on power systems 16 (3) (2001) 537–544.
[20] Smart Wires, Inc., Overview of Smart Wires Solutions, accessed: 2019-09-10 (2017).
URL https://www.electranet.com.au/wp-content/uploads/ritt/2016/11/Smart-Wires-submission.pdf
[21] M. Sahraei-Ardakani, S. A. Blumsack, Transfer capability improvement through market-based operation of series FACTS devices, IEEE Transactions on Power Systems 31 (5) (2015) 3702–3714.
[22] M. Sahraei-Ardakani, K. W. Hedman, Day-ahead corrective adjustment of FACTS reactance: A linear programming approach, IEEE Transactions on Power Systems 31 (4) (2015) 2867–2875.
[23] B. Stott, J. Jardim, O. Alsaç, DC power flow revisited, IEEE Transactions on Power Systems 24 (3) (2009) 1290–1300.
[24] T. Ding, R. Bo, F. Li, H. Sun, Optimal power flow with the consideration of flexible transmission line impedance, IEEE Transactions on Power Systems 31 (2) (2015) 1655–1656.
[25] M. Sahraei-Ardakani, K. W. Hedman, Computationally efficient adjustment of FACTS set points in DC optimal power flow with shift factor structure, IEEE Transactions on Power Systems 32 (3) (2016) 1733–1740.
[26] Y. Sang, M. Sahraei-Ardakani, M. Parvania, Stochastic transmission impedance control for enhanced wind energy integration, IEEE Transactions on Sustainable Energy 9 (3) (2017) 1108–1117.
[27] M. Sahraei-Ardakani, Y. Sang, Discussion on linear modeling of variable reactance in "co-optimization of transmission expansion planning and tcsc placement considering the correlation between wind and demand scenarios", IEEE Transactions on Power Systems 33 (5) (2018) 5808–5809.
[28] M. B. Shafik, H. Chen, G. I. Rashed, R. A. El-Sehiemy, Adaptive multi objective parallel seeker optimization algorithm for incorporating TCSC devices into optimal power flow framework, IEEE Access 7 (2019) 36934–36947.
[29] IEEE 118-bus, 54-unit, 24-hour system, accessed: 2021-07-05.
URL https://www.researchgate.net/file.PostFileLoader.html?id=568516485f7f71c9c68b456c&assetKey=AS%3A312690231185408%401451562568681
[30] A. B. Birchfield, T. Xu, K. M. Gegner, K. S. Shetye, T. J. Overbye, Grid structural characteristics as validation criteria for synthetic networks, IEEE Transactions on power systems 32 (4) (2016) 3258–3265.
[31] ACTIVSg2000: 2000-bus synthetic grid on footprint of texas, accessed: 2018-11-15 (2016).
URL https://electricgrids.engr.tamu.edu/electric-grid-test-cases/activsg2000/
[32] Y. Sang, M. Sahraei-Ardakani, Effective power flow control via distributed FACTS considering future uncertainties, Electric Power Systems Research 168 (2019) 127–136.
[33] Y. Sang, M. Sahraei-Ardakani, Economic benefit comparison of D-FACTS and FACTS in transmission networks with uncertainties, in: 2018 IEEE Power & Energy Society General Meeting (PESGM), IEEE, 2018, pp. 1–5.
[34] Power systems test case archive, accessed: 2020-06-15.
URL http://labs.ece.uw.edu/pstca/rts/pg_tcarts.htm
[35] J. Jin, Y. Xu, A flow direction enforcing approach for economic dispatch with adjustable line impedance, in: 2017 IEEE Power & Energy Society General Meeting, IEEE, 2017, pp. 1–5.

Appendix

Our method to increase the congestion level in the test systems is through reducing the thermal limit of lines that are utilized the most. For the 118-bus system, we first decrease the capacities of all lines by 20%. Then, some of the heavily utilized lines' capacities modified further, and the modifications are presented in Table 21.

The modifications for the 2000-bus system are presented in Table 22.

Table 21: Modifications of line capacities in the 118-bus system

Line num.	Line cap. (MW)	Modified line cap. (MW)
5	175	87.5
8	500	225
37	175	61.25
38	500	250
41	140	35
54	175	122.5
78	175	43.75
96	500	225
104	500	125
131	175	78.75
133	500	175
134	500	125
135	175	87.5

Table 22: Modifications of line capacities in the 2000-bus system

Line num.	Line cap. (MW)	Modified line cap. (MW)
43	149	112
58	170	128
71	145	109
74	149	112
112	230	200
364	82	62
435	143.8	108
439	83	62
556	230	172.5
557	230	172.5
558	250	213
765	168	145
935	2295	1721
1038	150	113
1222	1379	1035
1380	1450	1088
1381	1450	1088
2136	217.8	190
2449	1600	1200
2450	1600	1200
2453	523	392
2803	198	180
2911	280.8	220
2912	280.8	220
2913	280.8	220
2993	213	180
2994	213	180
2995	213	180